CrystEngComm

ROYAL SOCIETY OF CHEMISTRY

PAPER

View Article Online
View Journal | View Issue

Cite this: *CrystEngComm*, 2026, **28**, 1658

Extremely efficient host selectivity behaviour of stable di-(9-(*p*-chlorophenyl)xanthen-9-yl) peroxide towards *ortho*-xylene when crystallized from mixtures of the C_8H_{10} aromatic fraction of crude oil

Benita Barton, * Jarryd A. Vorgers and Eric C. Hosten

Herein we report on the host ability of di-(9-(*p*-chlorophenyl)xanthen-9-yl) peroxide (**H**) for the four isomers of the C_8H_{10} aromatic crude oil fraction, namely *o*-, *m*- and *p*-xylene (*o*-Xy, *m*-Xy and *p*-Xy) and ethylbenzene (EB). Crystallization of **H** from each of these solvents revealed that both *o*-Xy and *p*-Xy formed complexes with this host species, while *m*-Xy and EB were not enclathrated. ^{1}H-NMR spectroscopic analysis of the resultant solids demonstrated that the host : guest (H : G) ratios for the two complexes were 1 : 1 and 4 : 1, respectively. The host compound was subsequently crystallized from various equimolar and binary non-equimolar mixtures of these isomers, and a remarkable selectivity for *o*-Xy was observed. In fact, it was demonstrated that **H** has the ability to separate the 20/80 and 40/60 *o*-Xy/*m*-Xy as well as the 40/60, 50/50, 60/40 and 80/20 *o*-Xy/EB mixtures: extremely high selectivity coefficients (*K*), in favour of *o*-Xy, were calculated in each of these instances. This is an extraordinary finding given the difficulty of separating such mixtures by the more conventional fractional distillations owing to the comparable physical properties of these guest solvents. The two complexes as well as guest-free **H** were subjected to both single crystal X-ray diffraction and thermal analyses. The former technique demonstrated that the preferred guest species, *o*-Xy, was accommodated in the complex in discrete cavities, while disfavoured *p*-Xy experienced wide open channel occupation. This observation explains the affinity of **H** for the *ortho* isomer relative to *p*-Xy when guests competed, since enhanced thermal stabilities of complexes are associated with the former type of accommodation (isolated voids). Furthermore, *o*-Xy experienced nonclassical H-bonding with the host molecule, an interaction type not observed in the case of the *para* isomer. Additionally, from the thermal experiments, the *p*-Xy-containing inclusion compound, plausibly as a result of its retention in wide open channels, possessed an extremely low thermal stability at ambient temperature and pressure, while the complex with *o*-Xy, which occupied discrete cavities, was stable in analogous conditions.

Received 15th January 2026,
Accepted 5th February 2026

DOI: 10.1039/d6ce00042h

rsc.li/crystengcomm

1. Introduction

The xylene and ethylbenzene isomers (*o*-Xy, *m*-Xy, *p*-Xy and EB) are collectively known as the C_8H_{10} aromatic fraction of crude oil. These compounds were first isolated by the distillation of wood as long ago as in 1850.[1] However, more recently, catalytic reforming of petroleum naphtha and coal carbonization processes have been employed in order to produce mixtures of these compounds.[2,3] Mixed Xy streams are, additionally, furnished through the methylation of benzene or toluene in the presence of solid-state catalysts.[4] EB, on the other hand, is more usually produced through the reaction of benzene with gaseous ethylene, with an acid serving as the catalyst in this particular process.[5,6]

Since Xy/EB do present as mixtures in the chemical industry, these isomers require separation owing to their dedicated applications in further chemical processes. As examples, *o*-Xy serves as a building block towards phthalic anhydride, a prominent intermediate for a number of materials and drug actives while, similarly, the *meta* isomer is used to produce isophthalic acid, a central monomer during a copolymerization process to afford modified polyethylene terephthalate, the latter of which is derived from *p*-Xy.[7] EB, on the other hand, is largely used for the production of styrene, also a monomer, to ultimately be employed in the formation of ubiquitous polystyrene products and other plastics.[8] Owing to the extremely narrow

Department of Chemistry, Nelson Mandela University, PO Box 77000, Gqeberha (Port Elizabeth), 6031, South Africa. E-mail: benita.barton@mandela.ac.za

boiling range of these four solvents (136–144 °C), fractional distillations for their separation are tedious, costly and time-consuming. In fact, in an article in *Nature*, Sholl and Lively reported that if an alternative and effective separation strategy for these isomers was discovered, this would "change the world".[9] Currently, large quantities of limited, non-renewable fossil fuels are required in order to separate these isomers through fractional distillation, which renders this method unsustainable if not also ineffective. Therefore, alternative separatory methodologies are essential, and many scientists have explored other options. Some of these include simulated moving bed technologies, metal–organic frameworks, membranes and zeolites, to mention only a few.[10–14] These procedures, however, are oftentimes characterized by exorbitant costs and limited scalability.

Host–guest chemistry, a subcategory of the supramolecular chemistry field,[15,16] has been proposed as an attractive alternative separatory protocol for Xy/EB mixtures. This branch of science employs a host compound which possesses an enhanced selectivity for only one of the isomers in the mixture. Ideally, upon crystallization of the host species from the mixed Xy/EB solution, only one of the four solvents becomes enclathrated in the so-formed inclusion compound. This complex is readily isolated from the solution through vacuum filtration, which effectively separates the preferred isomer from the others, and the complexed guest may then be facilely liberated from the cavities of the complex through extremely mild heat. This separatory protocol for these isomers has been extensively explored in our own laboratories. As such, host compounds possessing two tricyclic fused systems synthesized from xanthone, thioxanthone, dibenzosuberone and dibenzosuberenone were all demonstrated to possess enhanced selectivities for, more usually, *p*-Xy, when crystallized from mixtures of these isomers, or *o*-Xy, dependent on the particular structure of the host molecule.[17–22] Additionally, (*R*,*R*)-(−)-2,3-dimethoxy-1,1,4,4-tetraphenylbutane-1,4-diol, derived from tartaric acid, also favoured *p*-Xy in the mixed guest crystallization experiments,[23] whilst host species having a roof-shaped geometry, prepared from anthracene and including the Diels–Alder addition reaction amongst others, similarly furnished complexes enriched in the *para* or *ortho* isomers.[24,25]

There exists an important need to explore other potential host compounds in an attempt to identify species with even greater selectivities than is currently observed in these crystallization experiments. To this end, the present investigation reports on the host behaviour of a peroxide compound, di-(9-(*p*-chlorophenyl)xanthen-9-yl) peroxide **H**, in the presence of these isomeric guest mixtures (Fig. 1). Mixed guest crystallization experiments were employed in order to ascertain whether **H** possesses preferential selectivity for a particular guest solvent in these mixtures. Moreover, any complexes that formed successfully were analysed by means of both single crystal X-ray diffractometry and thermal analysis in order to understand the host behaviour in the Xy/EB mixed guest experiments. Additionally, the crystal structure of guest-free **H** was also explored. We now report on all of these findings.

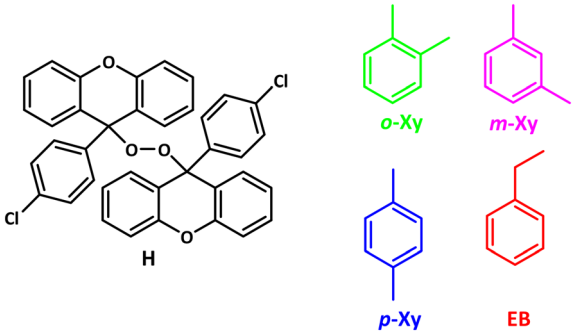

Fig. 1 The molecular structures of **H**, di-(9-(*p*-chlorophenyl)xanthen-9-yl) peroxide, and the four isomeric C_8H_{10} solvents (*o*-Xy, *m*-Xy, *p*-Xy and EB).

2. Experimental

2.1 General

The host compound **H** was synthesized using chemicals purchased from Merck (South Africa) and these were used as received. The C_8H_{10} isomers were also procured from Merck.

^{1}H-NMR experiments were carried using a Bruker Ultrashield Plus 400 MHz spectrometer; $CDCl_3$ was the deuterated solvent. Spectral data were analysed using Topspin 4.4.1 software.

The crystal structures of guest-free **H**, **H**·*o*-Xy and **H**·2(*p*-Xy) were obtained by employing a Bruker D8 Quest diffractometer, featuring a Photon II CPAD detector and IμS 3.0 Mo source (Kα, λ = 0.71073 Å). Diffraction data acquisition was by means of APEX4, and SAINT facilitated cell refinement and data reduction.[26,27] Absorption effects were accounted for by using the numerical correction method in SADABS.[26] Crystal structures were solved by employing the dual-space approach in SHELXT-2018/2[28] and subsequently refined through least-squares techniques in SHELXL-2019/3.[29] Graphical visualization was accomplished with SHELXLE,[30] and structural diagrams were created using ORTEP-3 for Windows (version 2023.1) (Fig. S1a–c in the SI).[31] Anisotropic refinement was applied to all non-hydrogen atoms, while carbon-bound hydrogen atoms were positioned according to standard geometric constraints (C–H bond lengths: 0.95 Å for aromatic carbons, 1.00 Å for methine and 0.99 Å for methylene) and refined using the riding model approximation, with U_{iso}(H) fixed at 1.2U_{eq}(C). Hydrogen atoms of the methyl groups were modelled with rotational freedom about the C–C bond to best match the experimental electron density (HFIX 137 in SHELXL[29] program). The U_{iso}(H) parameters were fixed at 1.5U_{eq}(C), with C–H bond lengths restrained to 0.98 Å. Hydroxyl hydrogen atoms were refined with rotational freedom about the C–O bond to achieve optimal fit with the experimental electron density (HFIX 147 in SHELXL[29] program). U_{iso}(H) was fixed at

$1.5U_{eq}$(O), with O–H bond lengths restrained to 0.84 Å. The crystal structures of these compounds (**H**, **H**·*o*-Xy and **H**·2(*p*-Xy)) were deposited at the Cambridge Crystallographic Data Centre, and their respective CCDC numbers are 2492472–2492474.

GC-MS analyses were carried out using a Young Lin YL6500 GC equipped with an Agilent J&W Cyclosil-B column (30 m × 250 μm × 0.25 μm, calibrated) coupled to a flame ionization detector. The method involved an initial 1 min hold time at 50 °C. A ramp rate of 10 °C min^{-1} was then implemented until a final temperature of 90 °C was reached, and this temperature was held there for 3 min. The flow rate was 1.5 mL min^{-1} and the split ratio 1 : 50. Due to instrument availability, an Agilent 7890A GC coupled to an Agilent 5975C VL mass spectrometer (GC-MS) equipped with the same column was also employed. The method involved an initial hold time of 1 min at 50 °C after which the sample was heated to 52 °C with a ramp rate of 10 °C min^{-1}. Finally, a heating rate of 0.3 °C min^{-1} was applied until a final temperature of 54 °C was attained. The flow rate was 1.5 mL min^{-1} and the split ratio 1 : 80.

2.2 Synthesis of di-(9-(*p*-chlorophenyl)xanthen-9-yl) peroxide (H)

The host compound was synthesised according to earlier reported procedures.[32–34]

2.3 Host crystallization experiments from each of the C_8H_{10} isomers

In order to determine whether **H** possessed host ability for each of the four potential guest isomers, crystallization experiments were performed in each one in glass vials. Therefore, **H** (0.05 g, 0.08 mmol) was dissolved in an excess of the solvent with mild heat being employed in order to ensure complete host dissolution. The vials were left open to the ambient temperature and pressure conditions, which facilitated some evaporation of the solvent, ultimately facilitating crystal formation. These were isolated from their solutions by means of vacuum filtration, washed with low boiling petroleum ether and analysed using ^{1}H-NMR spectroscopy. Enclathration was successful when both host and guest resonance signals were observed on the resultant spectrum. The host : guest (H : G) ratio was calculated by comparing the areas under applicable host and guest resonance signals.

2.4 Host crystallization experiments from equimolar guest mixtures

The host selectivity was subsequently investigated, also in glass vials, by crystallizing **H** from mixed guest solutions containing the guests in equimolar proportions; all possible guest combinations were considered. As such, **H** (0.05 g, 0.08 mmol) was dissolved in these equimolar mixed guests (5–7 mmol combined amount) and the vials were closed and stored at ambient conditions. The crystals that formed in this manner were isolated and treated as in the single solvent experiments. The guest ratios in any mixed complexes that formed were determined through GC analysis, while ^{1}H-NMR spectroscopy was applicable in order to calculate the overall H : G ratios.

2.5 Host crystallization experiments from binary guest solutions with differing molar ratios

Since mixed guests in the industry are, more usually, not equimolar in nature, the host compound was also crystallized from binary guest solutions but where the two guests present, G_A and G_B, were prepared in 20 : 80, 40 : 60, 60 : 40 and 80 : 20 molar ratios. These crystallizations were carried out in an identical fashion to the equimolar guest experiments. Analysis of the crystals was also by means of GC, which provided the guest amounts in the so-formed mixed guest complexes. Selectivity profiles were then constructed by plotting Z_A (or Z_B), the amount of G_A (or G_B) in the crystals, against X_A (or X_B), the amount of G_A (or G_B) in the original solution, according to the equation of Pivovar and colleagues, $K = Z_A/Z_B \times X_B/X_A$, where $X_A + X_B = 1$.[35] These plots provide a visual manner of observing the host selectivity behaviour in such changing guest quantities. K is the selectivity coefficient and may be calculated for each data point in these plots and serves as a measure of the host selectivity. It has been reported that K is required to be 10 or greater for effective separations of such binary mixtures.[36] When $K = 1$, the host compound is not selective; this eventuality is represented by the straight diagonal lines that have been inserted into each of these profiles.

2.6 Software

Program Mercury[37] was employed in order to analyse the crystal structures obtained from SCXRD analysis. This program facilitated the preparation of all unit cell, packing, noncovalent interaction and void diagrams. In the latter instance, the guest molecules were deleted from the packing calculations and the spaces that formed in this manner were then investigated by means of a probe with a 1.2 Å radius.

3. Results and discussion

3.1 Host crystallization experiments from each of the C_8H_{10} isomers

When **H** was crystallized from each of *o*-Xy, *m*-Xy, *p*-Xy and EB, two complexes were isolated, namely **H**·*o*-Xy (H : G 1 : 1) and 4(**H**)·*p*-Xy (4 : 1), while *m*-Xy and EB did not form inclusion compounds with this host species (the relevant ^{1}H-NMR spectra are provided in the SI, Fig. S2a–d).

3.2 Host crystallization experiments from equimolar guest mixtures

Since **H** possessed host ability for *o*- and *p*-Xy in the single solvent crystallization experiments, mixed guest crystallization experiments were feasible in order to ascertain whether **H** is selective in such conditions. Table 1 summarises the results

Table 1 The guest and overall H : G ratios of complexes formed in the equimolar guest mixtures[a]

o-Xy	*m*-Xy	*p*-Xy	EB	Guest ratios	Overall H : G ratios	% e.s.d.s
X	X			**90.4** : 9.6	1 : 1	1.9
X		X		**81.9** : 18.1	2 : 3	0.6
X			X	**95.3** : 4.7	1 : 1	0.9
	X	X		[b]	[b]	[b]
	X		X	[b]	[b]	[b]
		X	X	[b]	[b]	[b]
X	X	X		[b]	[b]	[b]
X	X		X	[b]	[b]	[b]
X		X	X	[b]	[b]	[b]
	X	X	X	[b]	[b]	[b]
X	X	X	X	**74.4** : 7.4 : 13.9 : 4.3	2 : 1	0.6 : 0.3 : 0.7 : 1.1

[a] Guest and overall H : G ratios were obtained through GC and ^{1}H-NMR experiments, respectively. [b] No guest solvent was detected in the solids emanating from these experiments.

that were obtained when **H** was crystallized from the various equimolar mixtures of these isomers. Experiments were carried out in duplicate to establish their repeatability and, thus, the percentage estimated standard deviations (% e.s.d.s) are also provided in this table. Furthermore, the preferred guest in each experiment is highlighted by means of bold text for ease of examination.

Interestingly, in the *m*-Xy/*p*-Xy, *m*-Xy/EB and *p*-Xy/EB binary experiments (*i.e.*, those without *o*-Xy present), as well as all ternary combinations of these guest solvents, only guest-free **H** was isolated (Table 1). However, *o*-Xy/*m*-Xy, *o*-Xy/*p*-Xy and *o*-Xy/EB (*i.e.*, where *o*-Xy was present) and also the quaternary guest solution, mixed guest complexes were recovered in each instance. Importantly, remarkable host selectivities were observed in both the *o*-Xy/*m*-Xy and *o*-Xy/EB solutions in favour of the *ortho* isomer, and 90.4 and 95.3% of this guest species were measured in the crystals, respectively. Furthermore, both the *o*-Xy/*p*-Xy and *o*-Xy/*m*-Xy/*p*-Xy/EB experiments also furnished mixed complexes enriched in *o*-Xy (81.9 and 74.4%). From the quaternary experiment, the host selectivity may be written as in the order *o*-Xy ≫ *p*-Xy > *m*-Xy > EB. Clearly **H** is extremely selective for *o*-Xy in the four experiments where mixed guest complexes were obtained. This isomer, together with *p*-Xy, is the more

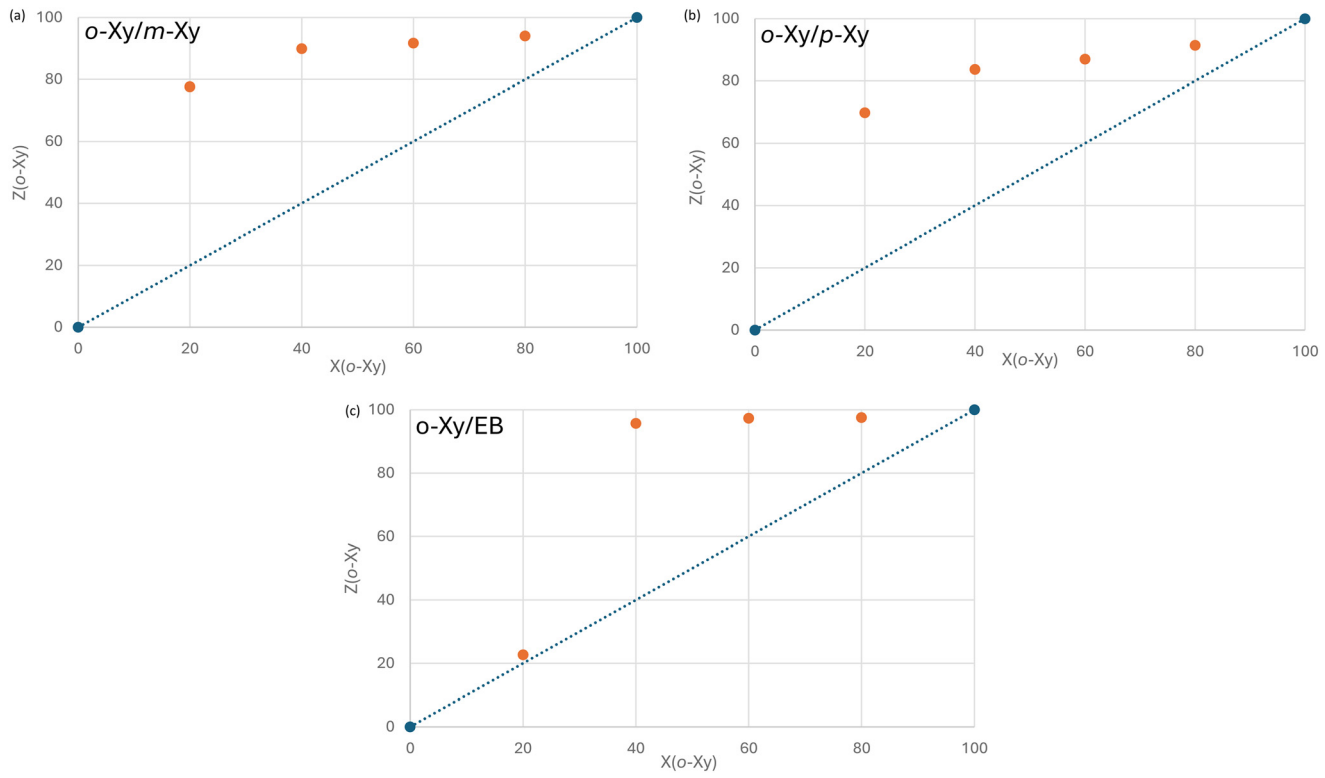

Fig. 2 Selectivity profiles of **H** when crystallized from the (a) *o*-Xy/*m*-Xy, (b) *o*-Xy/*p*-Xy and (c) *o*-Xy/EB binary mixtures. All other binary guest solutions produced only guest-free **H**.

Table 2 Calculated K values for **H** in the binary C_8H_{10} solutions

o-Xy percentage in the original solution	*o*-Xy/*m*-Xy	*K* values (in favour of) *o*-Xy/*p*-Xy	*o*-Xy/EB
20	**13.9** (*o*-Xy)	9.3 (*o*-Xy)	1.2 (*o*-Xy)
40	**13.4** (*o*-Xy)	7.7 (*o*-Xy)	**33.5** (*o*-Xy)
50	9.4 (*o*-Xy)	4.5 (*o*-Xy)	**20.3** (*o*-Xy)
60	7.4 (*o*-Xy)	4.5 (*o*-Xy)	**23.9** (*o*-Xy)
80	3.9 (*o*-Xy)	2.7 (*o*-Xy)	**9.8** (*o*-Xy)

usually favoured one of numerous host compounds investigated in our laboratories.[17–25] Finally, the overall H : G ratios varied from 1 : 1 and 2 : 3 to 2 : 1.

3.3 Host crystallization experiments from binary guest solutions with differing molar ratios

The selectivity profiles for the *o*-Xy/*m*-Xy, *o*-Xy/*p*-Xy and *o*-Xy/EB binary guest experiments are provided in Fig. 2a–c. Only these guest combinations furnished complexes, with all of the other binary mixtures affording guest-free host compound only. The selectivity coefficients for all data points contained in these plots are summarised in Table 2, with those approaching 10 or greater highlighted in bold text; these binary solutions in particular may be separated by means of supramolecular chemistry protocols.[36] The K values for the equimolar binary experiments from Table 1 have been calculated here as well, and these are also inserted into Table 2 (note that the preferred guest in every instance was *o*-Xy).

From Fig. 2a (*o*-Xy/*m*-Xy), it is clear that **H**, as expected given the results from the equimolar experiments, possesses an extremely high affinity for *o*-Xy when *m*-Xy was the other guest species, irrespective of its concentration in the binary solution. Crystals emanating from the 20, 40, 60 and 80% *o*-Xy mixtures contained 77.6, 89.9, 91.7 and 94.0% *o*-Xy. The K values that were calculated for these experiments ranged between 3.9 and 13.9 (Table 2). Two solutions may be separated using this strategy, those containing 20 and 40% *o*-Xy; K measured 13.9 and 13.4, respectively. In the remaining two solutions, the 60 and 80% *o*-Xy experiments, separations are not feasible owing to these experiments being characterised by low K values, 7.4 and 3.9. Furthermore, K was 9.4 for the 50% *o*-Xy experiment, and this too cannot be separated in this particular fashion.

Table 3 Crystallographic data for guest-free **H** and its complexes with *o*-Xy and *p*-Xy

	H	**H**·*o*-Xy	**H**·2(*p*-Xy)
Chemical formula	$C_{38}H_{24}Cl_2O_4$	$C_{38}H_{24}Cl_2O_4{\cdot}C_8H_{10}$	$C_{38}H_{24}Cl_2O_4{\cdot}2(C_8H_{10})$
Formula weight	615.47	721.63	827.79
Crystal system	Triclinic	Triclinic	Triclinic
Space group	$P\bar{1}$	$P\bar{1}$	$P\bar{1}$
μ (Mo-Kα)/mm^{-1}	0.270	0.230	0.198
a/Å	9.0084(3)	9.4967(3)	10.3526(4)
b/Å	9.1333(3)	9.9640(4)	10.6770(4)
c/Å	10.0681(3)	11.4322(4)	10.8850(4)
Alpha/°	101.0218(11)	64.5859(12)	111.158(1)
Beta/°	113.0514(10)	75.1697(12)	95.138(1)
Gamma/°	100.4349(10)	65.7342(11)	102.671(1)
V/Å^3	717.49(4)	886.59(6)	2417.08(18)
Z	1	1	1
F(000)	318	376	434
Temp./K	200	200	200
Restraints	0	54	0
N_{ref}	3561	4408	5332
N_{par}	200	262	274
R	0.0418	0.0380	0.0433
wR_2	0.1087	0.0984	0.1112
S	1.05	1.07	1.05
$\theta_{min-max}$/°	2.3, 28.3	2.4, 28.3	2.1, 28.3
Tot. data	58 346	73 285	71 327
Unique data	3561	4408	5332
Observed data [$I > 2.0$ sigma(I)]	3039	3704	4293
R_{int}	0.035	0.039	0.049
Completeness	1.000	0.998	0.999
Min. resd. dens./e/Å^3	−0.86	−0.39	−0.36
Max. resd. dens./e/Å^3	0.71	0.37	0.34
Density/g cm^{-3}	1.424	1.352	1.278

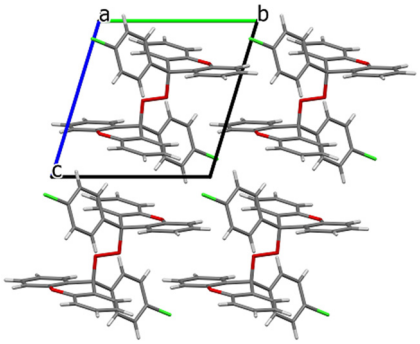

Fig. 3 Host packing and unit cell ([100]) of guest-free **H**.

Fig. 2b (*o*-Xy/*p*-Xy), once more, demonstrates that **H** remained consistently selective for *o*-Xy though, it must be said, this host affinity behaviour was somewhat lower than in the *o*-Xy/*m*-Xy experiments. The 20, 40, 60 and 80 *o*-Xy mixtures furnished complexes with 69.9, 83.7, 87.0 and 91.4% *o*-Xy. In each case, the calculated *K* value was too low (2.7–9.3) to present **H** as a possible host candidate for efficient separations of these solutions. This was also the case for the 50% *o*-Xy solution where *K* was calculated to be only 4.5.

Remarkable observations are evident from the selectivity profile depicted in Fig. 2c (*o*-Xy/EB). While the 20% *o*-Xy solution afforded a complex with only slightly elevated quantities of *o*-Xy (22.7%, K = 1.2), the remaining experiments saw a near-complete encapsulation of this guest species. From the 40, 60 and 80% *o*-Xy solutions crystallized complexes with as much as 95.7, 97.3 and 97.5% *o*-Xy. In the first two of these, *K* was extraordinary, 33.5 and 23.9, while in the last experiment (80% *o*-Xy), *K* approached 10 (9.8). Additionally, *K* was determined to be 20.3 for the 50% *o*-Xy experiment. Therefore, in all cases, with the exception of the 20% *o*-Xy solution, **H** would be an extremely effective host compound for such separations/purifications.

3.4 Single crystal X-ray diffractometry

Guest-free **H** and its complexes with *o*-Xy and *p*-Xy were subjected to SCXRD analysis. Table 3 contains the relevant crystallographic data for these experiments. All three crystalline solids crystallised in the triclinic crystal system and space group $P\bar{1}$. No disorder was evident in these structures with the exception of the guest in **H**·*o*-Xy, which experienced disorder around an inversion centre.

Fig. 3 depicts the unit cell and host molecule packing in guest-free **H**.

The molecular geometry of the host species was observed to possess an inversion centre in the midpoint of the O–O peroxide functionality. This geometry (Fig. 4, a stereoview) was maintained by means of an intramolecular C–H···π interaction (2.91 (H···π) and 3.836(2) (C···π) Å, 165°), whilst the packing was stabilized by a series of intermolecular interactions (Fig. 4, 2.87 and 2.91, 3.699(2) and 3.723(2) Å, 147 and 145°, respectively) of this kind and, additionally, intermolecular π···π close contacts as demonstrated in Fig. 5 (3.708(1) and 3.887(1) Å, with slippages of 1.198 and 1.990 Å).

Two weak hydrogen bonds were also identified in this crystalline solid, one intermolecular and the other intramolecular in nature. In the first of these were involved an aromatic hydrogen atom on the xanthenyl system and a chlorine atom on the free aromatic ring. Measurements were

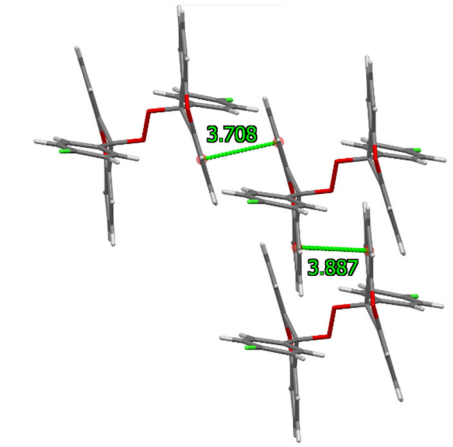

Fig. 5 The intermolecular π···π close contacts in guest-free **H**.

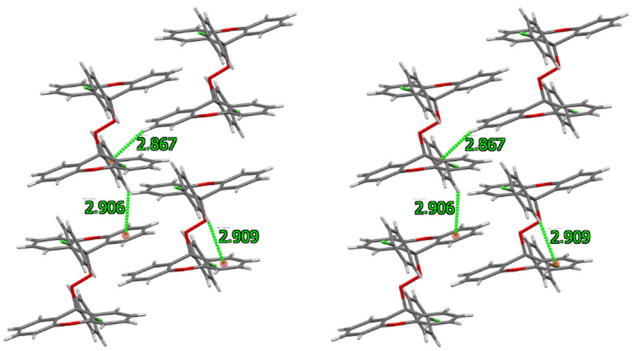

Fig. 4 A stereoview of the intra- and intermolecular C–H···π interactions in guest-free **H**.

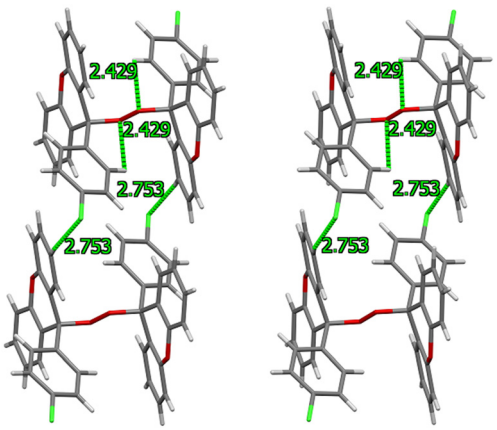

Fig. 6 A stereoview of the weak nonclassical C–H···Cl (intermolecular) and C–H···O (intramolecular) interactions present in guest-free **H**.

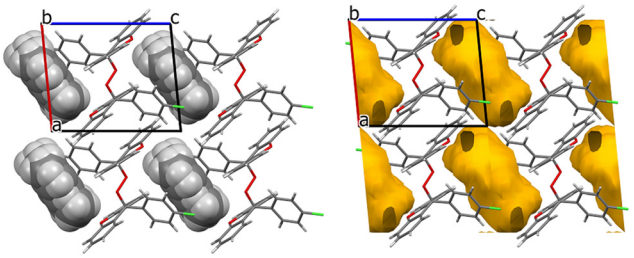

Fig. 7 The unit cell ([010]) and host–guest packing (left) and voids (right) in **H**·*o*-Xy. Guest and host molecules are in spacefill and stick representations, respectively.

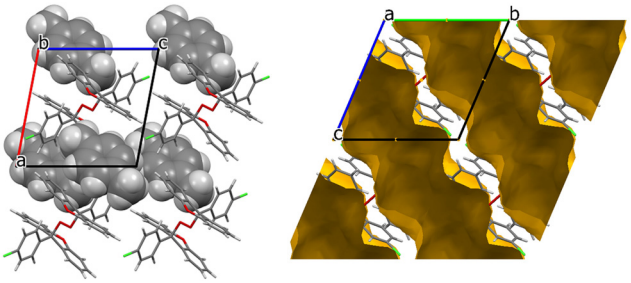

Fig. 9 Host–guest packing (left) and voids (right) in **H**·2(*p*-Xy). Guest and host molecules are in spacefill and stick forms, respectively.

2.75 (H···Cl) and 3.646(2) Å (C···Cl), and the bond angle was 157°. This is illustrated in Fig. 6 (a stereoview) together with the intramolecular close contact between an aromatic hydrogen atom on the free aromatic moiety and an oxygen atom of the peroxide functional group (2.43 (H···O) and 2.774(2) (C···O) Å, 101°).

The unit cell and host–guest packing in complex **H**·*o*-Xy is illustrated in Fig. 7 (left), while the void diagram after deleting the guest molecules from the packing calculation may be viewed on the right-hand side. These guest molecules occupied discrete cavities in the crystalline complex.

A singular intermolecular π···π interaction was observed between host molecules in this complex, together with one (host)C–H···π(host) close contact. Applicable measurements were 3.9792(10) Å (slippage 0.861 Å), and 2.95 and 3.7883(18) Å (148°). The guest molecule did not interact in this manner. Additionally, nonclassical hydrogen bonds were evident and involved a hydrogen atom of the free aromatic moiety and the oxygen of the peroxide group within the same molecule (2.46, 2.8124(16) Å, 102°), as well as another hydrogen on the free ring and the xanthenyl oxygen atom of a neighbouring host molecule (2.53, 3.392(2) Å, 151°). The guest molecules were also retained in the complex by means of nonclassical hydrogen bonds: here, a hydrogen atom of the methyl group of *o*-Xy interacted favourably with the host chlorine atom (Fig. 8). Measurements were 2.93 Å and 155°. This was the only host···guest close contact identified in this complex.

Fig. 9 (left, [010]) depicts the host–guest packing and unit cell, and the voids (right, [100]) for the complex containing *p*-Xy. Note that while the ^{1}H-NMR experiment suggested a 4 : 1 H : G ratio, this was observed to be 1 : 2 through SCXRD analysis. The discrepancy in these ratios is as a result of the extreme instability of this complex, as will be discussed in the Thermal analysis section.

Interestingly, the guest molecules in this complex resided in infinite channels rather than discrete cavities as was the case for *o*-Xy. This observation explains the affinity of **H** for *o*-Xy in the guest competition experiments: channel occupation by guest molecules is associated with decreased thermal stabilities of inclusion compounds while complexes in which guests are accommodated in discrete cavities are usually more stable (the thermal stability of the two complexes of the present investigation are reported in the Thermal analysis section that follows).

A scrutiny of the noncovalent interactions present in **H**·2(*p*-Xy) was subsequently undertaken. While no π···π interactions could be identified, the guest molecule experienced two (host)C–H···π(guest) close contacts involving both the host xanthenyl and free aromatic hydrogen atoms. Applicable measurements were 2.84 and 3.512(2) Å (129°), and 2.62 and 3.498(2) Å (154°). Furthermore, a (guest) C–H···π(host) interaction was also identified (2.85, 3.486(2) Å, with a bond angle of 125°). Two of these three interactions are depicted in Fig. 10 (a stereoview). Moreover, no nonclassical hydrogen bonds between the host and guest species (and, also, between host and host molecules) were

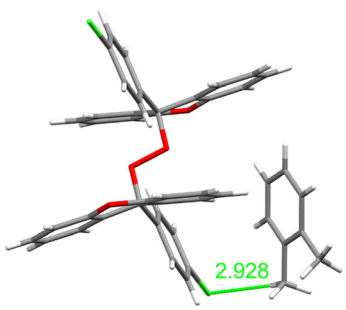

Fig. 8 (Guest)H_2C–H···Cl–C(host) interaction in the complex with *o*-Xy.

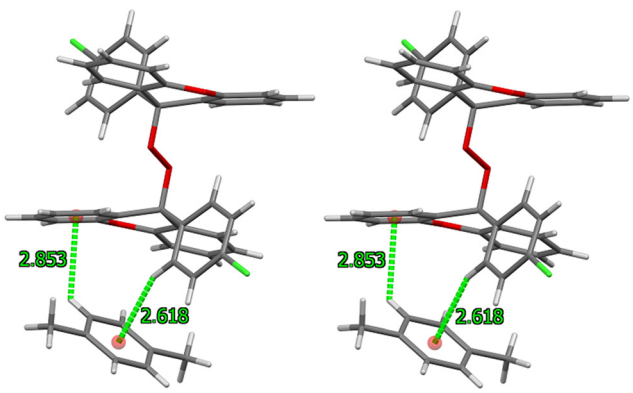

Fig. 10 Two of the three C–H···π contacts present in **H**·2(*p*-Xy).

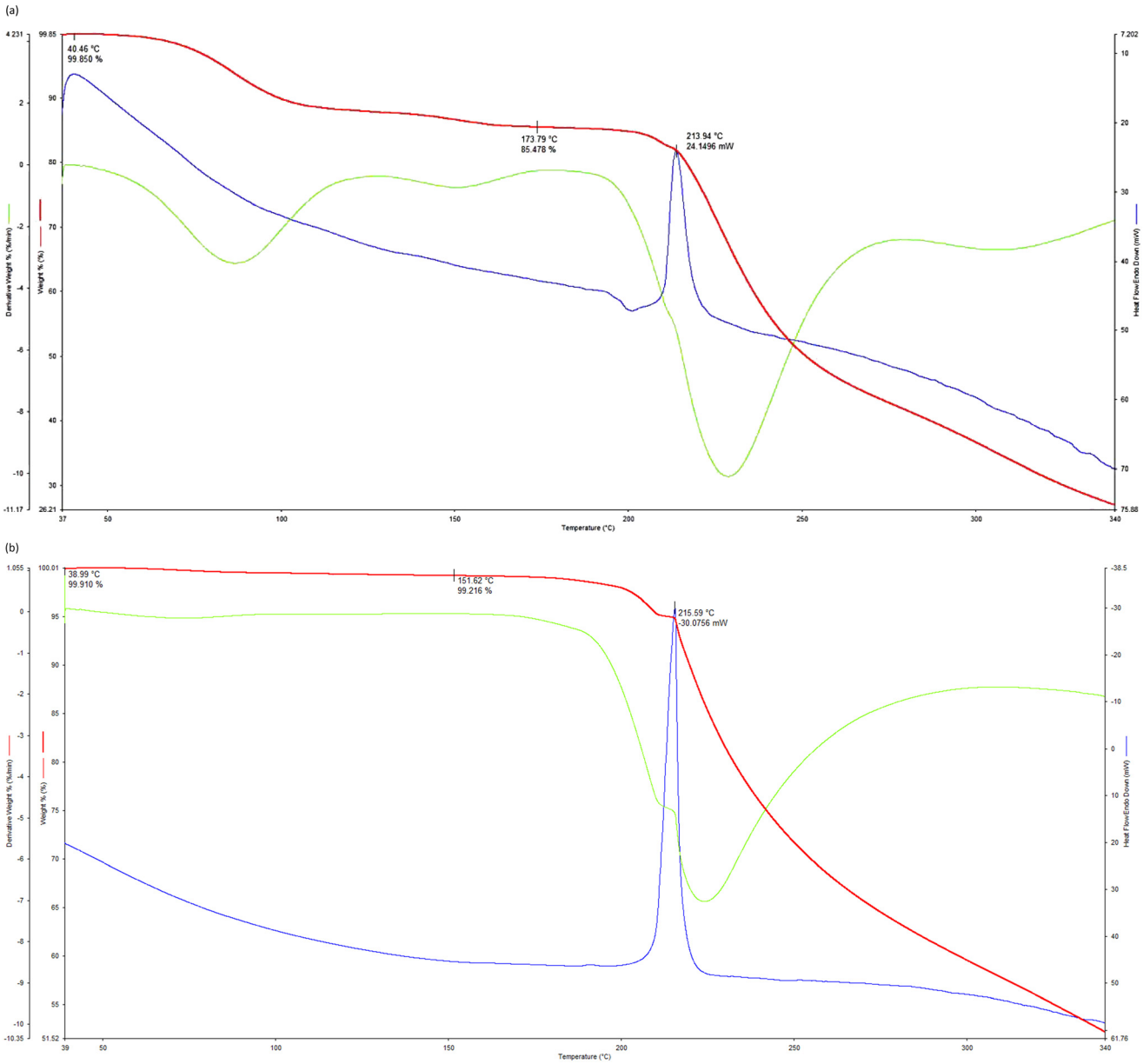

Fig. 11 The DSC (blue), TG (red) and DTG (green) traces for (a) H·*o*-Xy and (b) 4(H)·*p*-Xy.

noted in this complex (contrarily to the guest in **H**·*o*-Xy, which did interact in this manner with the host species); this observation may, together with the type of guest accommodation already discussed (discrete cavities *vs.* channels), provide a plausible reason for the host selectivity for the *ortho* isomer rather than *p*-Xy in the guest competition experiments.

3.5 Thermal analysis

The thermal traces that were obtained after thermal analysis on the two complexes produced in this work are provided in Fig. 11a and b. Here, the differential scanning calorimetric (DSC), thermogravimetric (TG) and its derivative (DTG) curves are overlaid in each one. The temperature at which the guest

Table 4 Thermal data for complexes of H formed with *o*-Xy and *p*-Xy[a]

Complex	T_{on}/°C	T_p/°C	Measured mass loss/%	Expected mass loss/%
H·*o*-Xy	40.5	213.9	14.4	14.7
4(**H**)·*p*-Xy	[b]	215.6	[b]	4.1

[a] T_{on} is the onset temperature for the guest release event and T_p is the peak temperature for the host decomposition. [b] T_{on} and the measured mass loss could not be determined owing to extreme instability of this complex at ambient conditions.

release event initiates (T_{on}) serves as a measure of the relative thermal stabilities for these complexes; these are summarised in Table 4 together with the experimental and expected mass losses, and the endotherm peak temperature (T_p) representing the decomposition of **H**.

The guest species in the complex **H**·*o*-Xy, upon being subjected to the heating program in this thermal experiment, escaped from the discrete cavities of the complex in two broad steps (Fig. 11a). T_{on} was 40.5 °C (Table 4). The measured and expected mass losses concurred closely (14.4 *vs.* 14.7%). However, a consideration of these traces for the *p*-Xy inclusion compound (Fig. 11b) revealed extreme instability at ambient conditions. Only 0.7% of the guest was observed to be lost in this experiment (the expected mass loss was 4.1%), with most of the release event occurring during sample preparation. T_{on} could also, as a consequence, not be measured. This observation is not entirely unexpected given the fact that *p*-Xy was accommodated in wide open channels in the crystals which facilitates facile guest escape (while the guest in **H**·*o*-Xy experienced discrete cavity occupation and was, as a result, more stable). Therefore, the preferred guest of **H** in the guest competition experiments, *o*-Xy, formed a complex that was significantly more stable than that containing the *para* isomer, a guest not favoured by **H**. These observations, once more, explain the selectivity behaviour of this host compound when presented with mixed guest solutions.

4. Conclusions

Di-(9-(*p*-chlorophenyl)xanthen-9-yl) peroxide (**H**), when crystallized from each of *o*-Xy, *m*-Xy, *p*-Xy and EB, formed inclusion compounds with *o*-Xy and *p*-Xy, while *m*-Xy and EB furnished only guest-free host compound. ^{1}H-NMR spectroscopy revealed that the H : G ratios of the complexes were 1 : 1 and 4 : 1, respectively. When the guest solvents were permitted to compete, it was observed, through GC analysis, that **H** possessed a remarkable selectivity for *o*-Xy. Furthermore, **H** was shown to have the ability to separate the 20/80 and 40/60 *o*-Xy/*m*-Xy solutions and, also, the 40/60, 50/50, 60/40 and 80/20 *o*-Xy/EB mixtures, since these experiments furnished remarkable selectivity coefficients in favour of *o*-Xy. These observations imply that, owing to the noteworthy *K* values calculated, such mixtures may be facilely separated on an industrial platform. Owing to such mixtures being extremely challenging to separate by means of fractional distillations as a result of their comparable physicochemical properties, these observations are extraordinary since they provide a much simpler, more efficient and significantly greener separatory strategy for such mixtures. SCXRD analyses were carried out on apohost **H** and its two complexes with *o*-Xy and *p*-Xy. This technique demonstrated that *o*-Xy, which was considerably preferred by the host species, experienced discrete cavity accommodation in the complex, while the *para* isomer (not favoured) was located in wide open and infinite channels. These observations explain the selectivity behaviour of **H**: complexes with their guests in discrete cavities possess, more usually, enhanced thermal stabilities compared with guests in wide open channels. Additionally, preferred *o*-Xy interacted with **H** through a nonclassical hydrogen bond, while this type of interaction in the inclusion compound containing the *para* isomer was not present. Finally, and expectedly (given the accommodation type), 4(**H**)·*p*-Xy, as demonstrated from thermal analysis, was exceedingly unstable at ambient conditions, quite plausibly as a result of the guest molecules being accommodated in wide open channels in the crystals of the complex. On the other hand, **H**·*o*-Xy, was significantly more stable since, here, the guest molecules resided in discrete cavity voids.

Author contributions

B. B.: conceptualization; methodology; funding acquisition; project administration; resources; supervision; visualization; writing the original draft. J. A. V.: investigation; methodology; validation; writing original draft. E. C. H.: data curation; formal analysis.

Conflicts of interest

There are no conflicts of interest to declare.

Data availability

Supplementary information (SI): the relevant ORTEP diagrams and ^{1}H-NMR spectra may be found in the SI. See DOI: https://doi.org/10.1039/d6ce00042h.

CCDC 2492472–2492474 (**H**, **H**·*o*-Xy and **H**·2(*p*-Xy)) contain the supplementary crystallographic data for this paper.[38a–c]

Acknowledgements

Financial support is acknowledged from the Nelson Mandela University and the National Research Foundation (NRF) of South Africa.

References

1 A. Cahours, Recherches sur les huiles légéres obtenues dans la distillation du bois (Investigations of light oils obtained by the distillation of wood), *Compte rendus*, 1850, **30**, 319–323.
2 M. R. Rahimpour, M. Jafari and D. Iranshahi, Progress in catalytic naphtha reforming process: A review, *Appl. Energy*, 2013, **109**, 79–93.
3 L. Ge, C. Zhao, S. Chen, Q. Li, T. Zhou, H. Jiang, X. Li, Y. Wang and C. Xu, *Energy*, 2022, **257**, 124779.
4 W. Deng, X. He, C. Zhang, Y. Gao, X. Zhu, K. Zhu, Q. Huo and Z. Zhou, Promoting xylene production in benzene methylation using hierarchically porous ZSM-5 derived from a modified dry-gel route, *Chin. J. Chem. Eng.*, 2014, **22**, 921–929.
5 J. C. Cheng, T. F. Degnan, J. S. Beck, Y. Y. Huang, M. Kalyanaraman, J. A. Kowalski, C. A. Loehr and D. N.

Mazzone, A comparison of zeolites MCM-22, beta, and USY for liquid phase alkylation of benzene with ethylene, *Stud. Surf. Sci. Catal.*, 1999, **121**, 53–60.

6 M. Lenarda, L. Storaro, G. Pellegrini, L. Piovesan and R. Ganzerla, Solid acid catalysts from clays: Part 3: Benzene alkylation with ethylene catalyzed by aluminum and aluminum gallium pillared bentonites, *J. Mol. Catal. A: Chem.*, 1999, **145**, 237–244.

7 J. Fabri, U. Graeser, T. Simo and A. Thomas, Xylenes, in *Ullmann's Encyclopedia of Industrial Chemistry*, Wiley-VCH, Weinheim Germany, 2000.

8 A. S. Fedotov, V. I. Uvarov, M. V. Tsodikov, S. Paul, P. Simon, M. Marinova and F. Dumeignil, Production of styrene by dehydrogenation of ethylbenzene on a [Re, W]/γ-Al_2O_3 (K, Ce)/α-Al_2O_3 porous ceramic catalytic converter, *Chem. Eng. Process.*, 2021, **160**, 108265.

9 D. Sholl and R. Lively, Seven chemical separations to change the world, *Nature*, 2016, **532**, 435–437.

10 D. Han, S. Wu, Z. Xia, R. Ao and L. Qi, Review: Advances in efficient separation of paraxylene from mixed xylene isomers using SMB technology and MOF materials, *J. Ind. Eng. Chem.*, 2025, **148**, 52–68.

11 Y. Liu, C. Wang, Q. Yang, Q. Ren and Z. Bao, Separation of xylene isomers using metal-organic frameworks: Addressing challenges in the petrochemical industry, *Coord. Chem. Rev.*, 2025, **523**, 216229.

12 F. P. McCandless and W. B. Downs, Separation of C_8 aromatic isomers by pervaporation through commercial polymer films, *J. Membr. Sci.*, 1987, **30**, 111–116.

13 L. Zhang, L. L. Li, N. J. Liu, H. L. Chen, Z. R. Pan and S. J. Lue, Pervaporation behaviour of PVA membrane containing β-cyclodextrin for separating xylene isomeric mixtures, *AIChE J.*, 2013, **59**, 604–612.

14 M. O. Daramola, A. J. Burger, A. Giroir-Fendler, S. Miachon and L. Lorenzen, Extractor-type catalytic membrane reactor with nanocomposite MFI-alumina membrane tube as separation unit: Prospect for ultra-pure para-xylene production from m-Xylene isomerization over Pt-HZSM-5 catalyst, *Appl. Catal., A*, 2010, **386**, 109–115.

15 J.-M. Lehn, *Supramolecular Chemistry Concepts and Perspectives*, VCH Verlagsgesellschaft mbH, Weinheim (Bundesrepublik Deutschland), 1st edn, 1995.

16 J. W. Steed and J. L. Atwood, *Supramolecular Chemistry*, Wiley, 3rd edn, 2022.

17 B. Barnardo, B. Barton, M. R. Caira and E. C. Hosten, Evaluation of the behaviour of two tricyclic-fused host systems in the presence of single and mixed isomers of the C_8H_{10} aromatic crude oil fraction, *Cryst. Growth Des.*, 2024, **24**, 5603–5613.

18 B. Barton, M. R. Caira, L. de Jager and E. C. Hosten, N,N′-Bis(9-phenyl-9-thioxanthenyl)ethylenediamine: highly selective host behavior in the presence of xylene and ethylbenzene guest mixtures, *Cryst. Growth Des.*, 2017, **17**, 6660–6667.

19 B. Barton, D. V. Jooste and E. C. Hosten, Synthesis and assessment of compounds *trans-N,N′*-bis(9-phenyl-9-xanthenyl)cyclohexane-1,4-diamine and *trans-N,N′*-bis(9-phenyl-9-thioxanthenyl)cyclohexane-1,4-diamine as hosts for potential xylene and ethylbenzene guests, *J. Inclusion Phenom. Macrocyclic Chem.*, 2019, **93**, 333–346.

20 B. Barton, U. Senekal and E. C. Hosten, Compounds *N,N′*-bis(9-cyclohexyl-9-xanthenyl)ethylenediamine and its thio derivative, *N,N′*-bis(9-cyclohexyl-9-thioxanthenyl)ethylenediamine, as potential hosts in the presence of xylenes and ethylbenzene: Conformational analyses and molecular modelling considerations, *Tetrahedron*, 2019, **75**, 3399–3412.

21 B. Barton, D. V. Jooste and E. C. Hosten, Behaviour of host compounds 1,2-DAX and 1,2-DAT in the presence of mixed xylene and ethylbenzene guest solvents, and comparisons with their 1,4 host derivatives, *J. Inclusion Phenom. Macrocyclic Chem.*, 2021, **100**, 155–167.

22 B. Barton, D. B. Trollip and E. C. Hosten, Selected tricyclic fused systems: Host behaviour in the presence of mixed xylenes and ethylbenzene, *Cryst. Growth Des.*, 2022, **22**, 6726–6734.

23 B. Barton, E. C. Hosten and P. L. Pohl, Discrimination between *o*-xylene, *m*-xylene, *p*-xylene and ethylbenzene by host compound (*R,R*)-(−)-2,3-dimethoxy-1,1,4,4-tetraphenylbutane-1,4-diol, *Tetrahedron*, 2016, **72**, 8099–8105.

24 B. Barton, U. Senekal and E. C. Hosten, Comparing the host behaviour of roof-shaped compounds *trans*-9,10-dihydro-9,10-ethanoanthracene-11,12-dicarboxylic acid and its dimethyl ester in the presence of mixtures of xylene and ethylbenzene guests, *CrystEngComm*, 2021, **23**, 4560–4572.

25 B. Barton, B. Barnardo and E. C. Hosten, Selectivity behaviour of two roof-shaped host compounds in the presence of xylene and ethylbenzene guest mixtures, *CrystEngComm*, 2021, **23**, 7278–7288.

26 A. Bruker, *APEX2, SADABS and SAINT*, Bruker AXS Inc., Madison (WI), USA, 2010.

27 Bruker, *APEX4, SADABS and SAINT*, Bruker AXS Inc., Madison, Wisconsin, USA, 2012.

28 G. M. Sheldrick, SHELXT - Integrated space-group and crystal-structure determination, *Acta Crystallogr., Sect. A: Found. Adv.*, 2015, **71**, 3–8.

29 G. M. Sheldrick, Crystal structure refinement with SHELXL, *Acta Crystallogr., Sect. C: Struct. Chem.*, 2015, **71**, 3–8.

30 C. B. Hübschle, G. M. Sheldrick and B. Dittrich, ShelXle: a Qt graphical user interface for SHELXL, *J. Appl. Crystallogr.*, 2011, **44**, 1281–1284.

31 L. J. Farrugia, WinGX and ORTEP for Windows: An update, *J. Appl. Crystallogr.*, 2012, **45**, 849–854.

32 B. Taljaard, The synthesis and reactions of stable peroxides, *PhD*, University of Port Elizabeth, Port Elizabeth, 1986.

33 B. Taljaard, A. Goosen and C. W. McCleland, Synthesis of hydrogen peroxide: Acid-catalysed decomposition of 9-hydroperoxy-9-phenylxanthene and its derivatives, *S. Afr. J. Chem.*, 1987, **40**, 139–145.

34 S. A. Glover, A. Goosen, C. W. McCleland, B. Taljaard and F. R. Vogel, Benzophenone-sensitized photo-oxidation of 9-phenylxanthene analogues, *S. Afr. J. Chem.*, 1985, **38**, 203–206.

35 A. M. Pivovar, K. T. Holman and M. D. Ward, Shape-selective separation of molecular isomers with tunable hydrogen-bonded host frameworks, *Chem. Mater.*, 2001, **13**, 3018–3031.
36 N. M. Sykes, H. Su, E. Weber, S. A. Bourne and L. R. Nassimbeni, Selective enclathration of methyl- and dimethylpiperidines by fluorenol hosts, *Cryst. Growth Des.*, 2017, **17**, 819–826.
37 C. Macrae, I. Sovago, S. Cottrell, P. Galek, P. McCabe, E. Padcock, M. Platings, G. Shields, J. Stevens, M. Towler and P. Wood, Mercury 4.0: From visualization to analysis. Design and prediction, *J. Appl. Crystallogr.*, 2020, **53**, 226–235.
38 (*a*) CCDC 2492472: Experimental Crystal Structure Determination, 2026, DOI: 10.5517/ccdc.csd.cc2pnmbb; (*b*) CCDC 2492473: Experimental Crystal Structure Determination, 2026, DOI: 10.5517/ccdc.csd.cc2pnmcc; (*c*) CCDC 2492474: Experimental Crystal Structure Determination, 2026, DOI: 10.5517/ccdc.csd.cc2pnmdd.